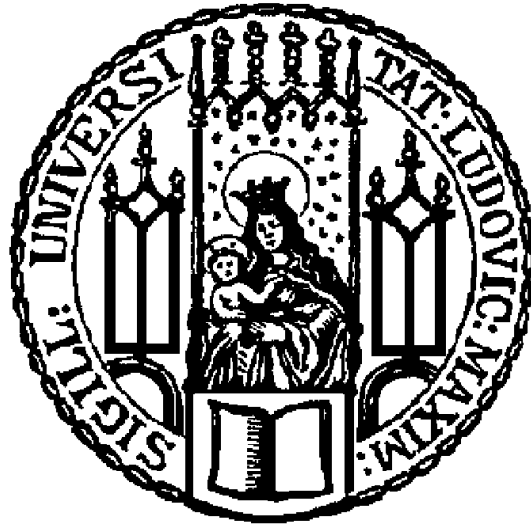


# Ludwig-Maximilians-Universität

München



## Tunneln von Elektronen zwischen normalen und helicalen 1D Kabeln mittels eines Quantenpunktes

Bachelorarbeit

Andreas Niklas Rank

Matrikel-Nummer 11414432

**Erstprüfer** Prof. Dr. Jan von Delft  
**Zweitprüfer** Dr. Oleg Yevtushenko  
**Betreuer** Dr. Oleg Yevtushenko



# Ludwig-Maximilians-Universität

München



Tunneling of electrons between normal and helical 1D wires  
coupled via a quantum dot

Bachelorarbeit

Andreas Niklas Rank

Matrikel-Nummer 11414432

**Erstprüfer** Prof. Dr. Jan von Delft  
**Zweitprüfer** Dr. Oleg Yevtushenko  
**Betreuer** Dr. Oleg Yevtushenko



# Contents

1	Introduction	5
1.1	The Quantum Spin Hall Effect or Two-Dimensional TR-invariant Topological Insulator and Helical Edge States . . . . .	6
1.2	Helical States in interacting Wires . . . . .	7
1.3	The Quantum Dot . . . . .	10
2	Statement of the Problem	11
3	Main Part	12
3.1	Rate Equations . . . . .	12
3.2	Solution of rate equations for different setups in equilibrium . . . . .	14
3.3	Solution of rate equations for different setups out of equilibrium . . . . .	19
4	Conclusion	23
5	Appendix: Calculation of $P_{\uparrow}, P_{\downarrow}$ and $P_0$	24
6	Acknowledgements	26
	Bibliography	27

## Abstract

This thesis addresses physics of helical electrons, which can be realized in 2D time-reversal (TR)-invariant topological insulators or interacting 1D wires. The helical electrons are protected against effects of local disorder due to the lock in relation between their momentum and spin, as long as the TR-symmetry is not violated. I examine tunneling between 1D helical and normal wires coupled via a quantum dot for different setups. Possible setups are two normal wires, a normal and a helical wire and two helical wires connected via the quantum dot. I derive rate equations for probabilities of electrons with an explicit spin state to be in the quantum dot ground state. These systems of equations are solved in the case of equilibrium and for the case where one wire is biased. Zero magnetization is found for the setups in the case of equilibrium. In the systems with biased helical wires, a finite magnetization appears. Detecting such a magnetization can be used in real experiments to identify the helical wires.

# 1 Introduction

Edges of Quantum Spin Hall samples support the so-called helical electrons, which have a lock-in relation between their momentum and spin. As one example, these edges arise in two-dimensional (2D) topological insulators (TI), which are insulating in the bulk but support a current at their edges. These states exist in the case of 2D TI due to the combination of spin-orbit coupling and time-reversal symmetry (T) [1]. Helical states (HS) are of very high interest in theoretical and experimental studies because they are protected against effects of local disorder as long as the TR-symmetry is not violated. One direction is to investigate on the helical wires (HW) connected to other quantum-devices, for example a quantum dot (QD) [2].

I investigate the tunneling of electrons between normal and helical 1D wires coupled via a QD. The thesis is structured into three parts. In the first part, I review different systems in which the HS emerge and experimental results for them. In the main part I introduce three setups of normal and helical wires connected via the QD and derive rate equations, which describe tunneling of electrons between the wires and the QD. I calculate the probabilities for electrons with an explicit spin in the QD through the sets of rate equations in the case of equilibrium and for biased wires. The conclusion, presented in the last part, summarizes the obtained results and shows further investigation possibilities regarding these systems of coupled wires.

## 1.1 The Quantum Spin Hall Effect or Two-Dimensional TR-invariant Topological Insulator and Helical Edge States

The Quantum Spin Hall insulator or 2D TR-invariant TI is a non-trivial topological phase of matter which possesses time-reversal symmetry  $T$  and protected edge states at the boundary. The 2D TI was first suggested by C.L.Kane and E.J.Mele in 2005 [3].

The key to the description of the 2D TI is the time-reversal symmetry which can be represented as an antiunitary operator  $\hat{\Theta} = e^{i\pi\hat{S}_y/\hbar}\hat{K}$ , with  $i$  is the imaginary unit,  $\hat{S}_y = \frac{\hbar}{2}\hat{\sigma}_y$  is the spin operator, ( $\hat{\sigma}_y$  is the second Pauli-matrix) and  $\hat{K}$  is the complex conjugation. For spin- $\frac{1}{2}$  fermions  $\hat{\Theta}^2 = -1$ , which leads to Kramer's degeneracy theorem stating that all eigenstates of a time-reversal invariant Hamiltonian are at least twofold degenerate. A time-reversal invariant Hamiltonian satisfy's  $\hat{\Theta}\hat{H}(k)\hat{\Theta}^{-1} = \hat{H}(-k)$  which holds for the special points at  $k = 0, \frac{\pi}{a}, -\frac{\pi}{a}$ , called Kramer's points.

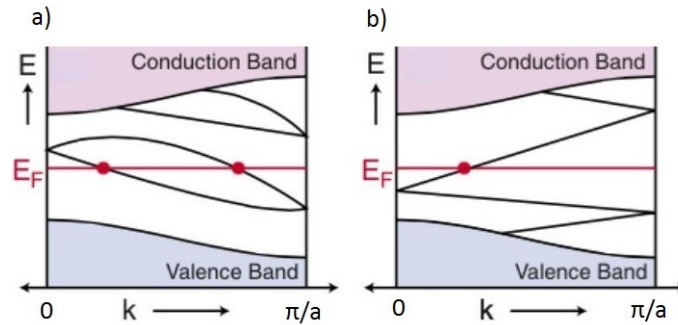


**Figure 1.1:** Panels (a) and (b) show the band structure with edge states of a 2-D TI in half of the brillouin zone (the other half is just a mirror image of this side due to the time reversal symmetry). The red line is the Fermi energy,  $E_F$ . The number of edge states at  $E_F$  can be even [panel (a)] or odd [panel (b)], see also Fig. 1.6 in Ref. [4].

Spin orbit interactions (SOI) split the spin degenerate bands of the Hamiltonian. Only the Kramer's points stay degenerate due to the mentioned theorem. If the number of edge states intersecting  $E_F$  is even, Fig.1.1 (a), one can push all edge states out of the energy gap through smoothly tuning the Hamiltonian. This system is then a conventional insulator. But if the number of edge states intersecting  $E_F$  is odd, Fig.1.1 (b), it is not possible to push all edge states out of the gap. This difference can be seen by looking at the topological class of the bulk structure. TR-symmetry ensures that every electron with momentum  $k$  has a partner at  $-k$ . This relates the number of Kramer's pairs modulo 2



## 1 Introduction

with a topological number, the  $\mathbb{Z}_2$  invariant. Thus, the 2D TI has topological protected edge states.

It has been predicted that the Quantum Spin Hall insulator can exist in HgTe/CdTe quantum wells, where a thin layer of HgTe is sandwiched by CdTe crystals. The system would be a trivial insulator for the thickness of the quantum well  $d_{QW} < d_c$  and a Quantum Spin Hall insulator, with helical edge states, for  $d_{QW} > d_c$ . Thus, the system undergoes a quantum phase transition from the trivial to the topological insulator at  $d \rightarrow d_c$ , with  $d_c$  being a critical thickness. A robust conductance with nearly the value  $2e^2/h$  has been measured which has not increased with the sample width, indicating it is caused by edge states. This conductance was suppressed by a small external field which violates TR-symmetry [5]. First measurements in the HgTe/CdTe structures were done by König et al., who detected the helical edge states (HES) of the 2D topological insulator at  $d_{QW} = 6.3nm$ .

## 1.2 Helical States in interacting Wires

Helical states (HS) can emerge not only as edge states of topological insulators but also in interacting 1d systems

For example, HS arise through a spontaneous breaking of the helical symmetry in a Kondo chain [6], [7], a one dimensional electron gas interacting with a lattice of dynamic spin impurities (Kondo) [8]. It has been predicted that two different phases can emerge in a regime of a sufficiently high density of spins, a band of electrons being far from half filling, and coupling constants  $J_x = J_y \equiv J_\perp$  isotropic in the XY plane. One phase with the anisotropy  $J_z > J_\perp$ , called easy axis (EA); and another phase with the anisotropy  $J_z < J_\perp$ , called easy plane (EP). All quasiparticle excitations are gapped in the case of the EA phase. Transport in this case is supported by charge density waves, a ground-state of one-dimensional electron gases transporting charges, [9]. These waves are not protected against local disorder: coupling with local impurities pins the charge transport. The transition of one phase to the other is a quantum phase transition at the SU(2) symmetric point  $J_z = J_\perp$ . The EP phase shows completely different transport properties as the minimum of the ground-state's energy corresponds to a helical spin-configuration, Fig.1.2 (c), opening a

## 1 Introduction

gap in the spectrum of the fermions of a particular helicity while the electrons with the opposite helicity remain gapless, Fig.1.2 (a), (b).

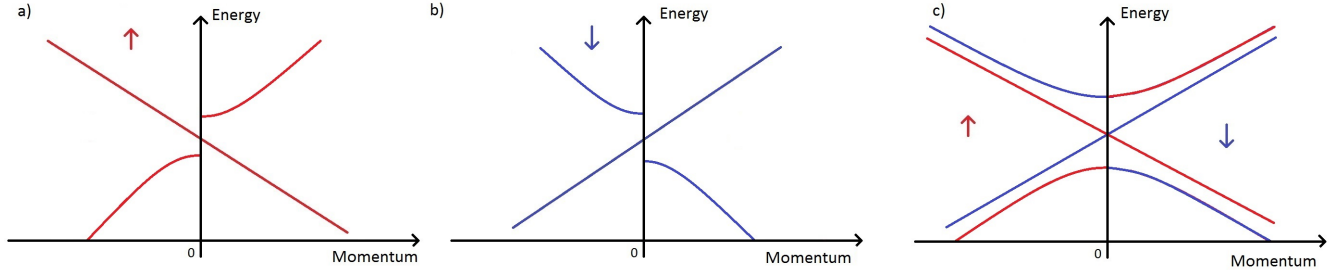


**Figure 1.2:** The partial gap opening is shown in panel (a) and (b). In (a) the gap opens for the spin- $\uparrow$  helical branch and in (b) for the spin- $\downarrow$  helical branch. Panel (c) shows the resulting dispersion relation.

This is the spontaneous breaking of the  $\mathbb{Z}_2$  helical symmetry, since every electron at momentum  $k$  should have a partner at momentum  $-k$  with the opposite spin. Transport is protected against local disorder either by spin-conservation (for electrons with the same helicity) or by the gap of one of the helical sectors (for electrons with a different helical symmetry). This protection of one-dimensional states due to the interactions is similar to the protection against local disorder at the edges of two-dimensional topological insulators [7].

A different and already experimentally investigated method for obtaining one-dimensional wires with the helical states is modulating the band-structure of a quantum wire so that a spin-orbit gap, a gap in the band-structure opened through SOI, Fig.1.3 (c), emerges. It can be measured in the linear conductance of the wire, such a gap can be obtained in the following way: We start with a spin-degenerate 1D sub-band, Fig.1.3 (a), and add the spin-orbit interaction (SOI)  $H_{SO} = \beta\sigma \cdot (k \times \nabla V)$ ,  $\beta$  is a material-dependent constant,  $\sigma$  is the particle's spin,  $k$  is the particle's momentum and  $V$  is the electrostatic potential. The SOI term splits the degenerate band into two spinful sub-bands, Fig.1.3 (b). This shift in the band-structure can not be measured through the conductance of the system and the value  $G_0 = 2e^2/h$  ( $e$  is the elementary charge and  $h$  is the Planck constant) of the original band remains. If a magnetic field is applied perpendicular to the one which lifted the spin-degeneracy, it can remove the degeneracy at the crossing point, Fig.1.3 (c). As this anti-crossing point is obtained, electrons with a spin- $\downarrow$  propagate with a positive momentum and electrons with a spin- $\uparrow$  propagate with a negative momentum for the lower band. This leads to the protection against local disorder: backscattering between the

## 1 Introduction

two bands must be accompanied by a spin-flip. If the Fermi energy lies inside the gap the conductance is reduced to  $G_0/2$  [10]. C. H. L. Quay et al. explored the spin-orbit gap in GaAs/AlGaAs quantum wires [10].

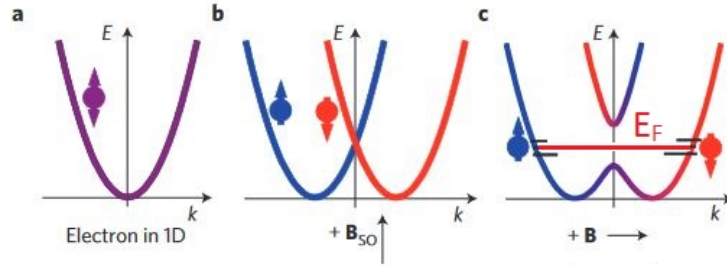


**Figure 1.3:** Panel (a) shows a spin-degenerate sub-band of a one-dimensional quantum wire. Panel (b) shows the sub-band shifted through the SOI to two spinful sub-bands.  $B_{SO} \uparrow$  stands for the applied magnetic field perpendicular to the wire. Panel (c) shows the so called spin-orbit gap achieved through a magnetic field  $B \rightarrow$  applied perpendicular to  $B_{SO} \uparrow$ , cf. Fig.1 in [10].

Possible evidence for the helical edge states was although given by C. P. Scheller et al. in Ref. [11] who measured the conductance of GaAs quantum wires in different temperature regimes. At temperatures  $T \gtrsim 10K$  the conductance of the wire reached  $2e^2/h$  as expected. Lowering the temperature leads to a reduction of the conductance to  $1e^2/h$  which becomes T independent at  $T \lesssim 0.1K$ . This was seen for many wires. A moderate magnetic field could not alter the conductance. A possible explanation was suggested in Ref. [12], where the formation of the helical phase due to the hyperfine interaction was considered. The theory says that the conductance of GaAs-based quantum wires is reduced with exactly the factor 2 as the nuclear spins form a helical order through their interactions with the electron system if the temperature is dropped below a crossover temperature. The helical spin order creates a field acting back on the electron's spin and leads to a partial gap opening following the helical order of the nuclei and dropping the conductance to a half. The authors of [11] stated that the theory of [12] is the only one which is able to explain their results. On the other hand, the direct proof of the helical transport was not been presented and is still absent.

### 1.3 The Quantum Dot

In this section I review basic knowledge about the quantum dot (QD), which will be used as a connection element in the setups of helical and normal wires.

Semiconductor heterostructures made of  $GaAs$  and  $Al_xGa_{1-x}As$  are used to create a two-dimensional electron gas, [13]. This electron gas exists due to the bigger band-gap of  $Al_xGa_{1-x}As$  between the insulating and the conducting band. The electrostatic potential in this heterostructure is lower near the surface as elsewhere close to it in the structure and so the electrons gather there forming a 2D electron gas. This gas is moving freely in the plane of the surface and is confined in the transverse direction cf. Ref. [14], pages 14-17. Through tailoring the sample of heterostructures with electrostatic confinement, induced with the help of metal gates, one can form a finite-size sample with controllable parameters like size and shape, [15]. A QD appears when one considers only zero mode (a kind of homogenous dynamics) inside these confined samples. The spatial scale of the QD is so small that electrons have discrete energy levels. They are like the energy levels of electrons in a box with a ground-state at the bottom and excited states at higher energies. Due to the Pauli exclusion principle, two or more identical fermions can not occupy the same quantum mechanical state. Thus, two electrons can occupy the same energy state of the QD if they have different spins.

In general, a QD can contain more than one degenerate energy level depending on the size of it and, therefore, it is necessary to think about electron-electron interactions. During the current project, we will make a simplification and consider a QD which can contain only one electron at a time. So electron-electron interactions will not be considered. Another simplification is that the gap between the first and the second energy level is very large and, therefore, the second level is assumed to be empty. Tunneling events, which take place between the QD and the different wires, have no restrictions.

## 2 Statement of the Problem

HS are a very hot modern topic in physics because of their protected ideal transport, which makes them very interesting for spintronics [10] and electronic semiconductor devices and quantum computing [1], [16]. A smoking gun evidence of their existence in 1D wires was not confirmed yet and so experimental ways and devices for their identification are still needed.

In the following I focus on the connection of helical wires with normal or helical wires via a QD.

The goal of the thesis is to investigate, whether setups of helical and normal wires magnetize the quantum dot if the systems are in the equilibrium and out of equilibrium. I although investigate, if a magnetization is obtained or changed if the tunneling rates are set to different limits.

If the QD magnetization depends on helicity of one (or both) connected wires, it can be used in real experiments to detect the HS.

# 3 Main Part

In this section, I derive and explain rate equations, cf. Ref. [17], for different setups of normal and helical wires connected via a QD. In the main part, I first derive the rate equations for a generic system of two wires connected via a QD. Then I calculate the magnetization in the case of equilibrium and out of equilibrium for the different setups.

## 3.1 Rate Equations

The main idea of the rate equations is to describe the occupation of the QD with electrons in a given spin-state. Tunneling of electrons between the wires and the QD is changing this occupation. Through the rate equations we are able to calculate the magnetization of the QD.

A model for a generic system, Fig.3.1, illustrates the different rates, which are derived in the following.

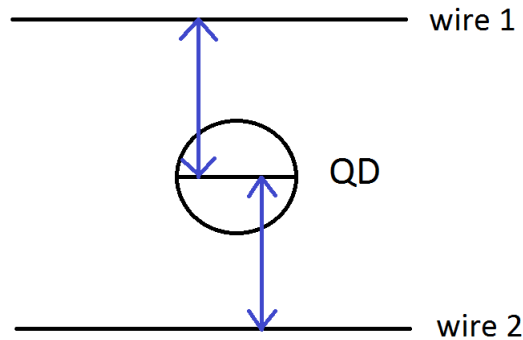


**Figure 3.1:** A scheme of two wires connected via the quantum dot. The blue arrows represent the tunneling electrons from a wire in the quantum dot or out of the quantum dot to a wire.

### 3 Main Part

To accomplish the calculation of the magnetization, we need probabilities  $P_\sigma$ , ( $\sigma \in [\uparrow\downarrow]$ ):  $P_\uparrow$  is the probability for an electron in the QD with spin- $\uparrow$  and  $P_\downarrow$  is the probability for an electron in the QD with spin- $\downarrow$ . The parameter  $P_0$  is the probability to have an unoccupied QD. The simple relation

$$P_0 = 1 - (P_\uparrow + P_\downarrow), \quad (3.1)$$

holds true. Tunneling events of electrons into the QD from a wire (in) and from the QD to a wire (out) are described by the rates  $\gamma_{wire_j}^{in,out}$ , with  $j \in [1, 2]$  the two different wires. An electron in the QD can spontaneously flip its spin, interacting with the QD nuclei. The rate  $\gamma_S$  is used for both a spin up-flip ( $\downarrow$  to  $\uparrow$ ) and a spin down-flip ( $\uparrow$  to  $\downarrow$ ), as there is no preference for one of these events in our setups.

The magnetization of the QD through electrons is a dynamical processes- It will be found by using the rate equations for the time derivatives of  $P_\uparrow$ ,  $P_\downarrow$  and  $P_0$ .

$$\partial_t P_\uparrow = (\gamma_{wire_1}^{in} + \gamma_{wire_2}^{in})P_0 - (\gamma_{wire_1}^{out} + \gamma_{wire_2}^{out})P_\uparrow + \gamma_S(P_\downarrow - P_\uparrow) \quad (3.2)$$

$$\partial_t P_\downarrow = (\gamma_{wire_1}^{in} + \gamma_{wire_2}^{in})P_0 - (\gamma_{wire_1}^{out} + \gamma_{wire_2}^{out})P_\downarrow + \gamma_S(P_\uparrow - P_\downarrow) \quad (3.3)$$

$$\begin{aligned} \partial_t P_0 = & (\gamma_{wire_1}^{out} + \gamma_{wire_2}^{out})P_\uparrow + (\gamma_{wire_1}^{out} + \gamma_{wire_2}^{out})P_\downarrow \\ & - (\gamma_{wire_1}^{in} + \gamma_{wire_2}^{in} + \gamma_{wire_1}^{in} + \gamma_{wire_2}^{in})P_0 \end{aligned} \quad (3.4)$$

The probability  $P_\sigma$  increases by tunneling of electrons with a given spin- $\sigma$  into the QD from the two wires and decreased by electrons with this spin tunneling out of the QD to the two wires. This is reflected by positive and negative contribution of the rates to Eq.(3.2) and Eq.(3.3). The probability  $P_0$  increases by tunneling into the QD and decreases by tunneling out of the QD regarding to no given spin state of the electrons. This is reflected by positive and negative contribution of all in and out tunneling rates to Eq.(3.4). The in-tunneling rates are always added with  $P_0$  as the electrons can only tunnel in the QD with it is not already occupied. The out-tunneling rates are added with  $P_\sigma$  regarding to the spin of the tunneling electrons as only electrons can tunnel out if the QD is occupied. The term  $\gamma_S P_\uparrow$  is subtracted as the probability for spin- $\uparrow$  electrons decreases if the spin-flips down, while the exact opposite holds for the  $\gamma_S P_\downarrow$  term. Spin flipping processes do not change the occupation of the quantum dot and do not contribute to  $P_0$ . But they change  $P_\sigma$ , a up-flip

### 3 Main Part

increases  $P_\uparrow$  and decreases  $P_\downarrow$ . A down-flip increases  $P_\downarrow$  and decreases  $P_\uparrow$ . The rates are added to the equations as explained.

Note that

$$\partial_t P_0 = -(\partial_t P_\uparrow + \partial_t P_\downarrow). \quad (3.5)$$

, due to Eq.(3.1). Plugging in Eq.(3.2) and Eq.(3.3) yields exactly Eq.(3.4).

## 3.2 Solution of rate equations for different setups in equilibrium

### Normal wire-normal wire setup (NW-NW)

In the first step, I investigate two normal wires coupled via the quantum dot. In the equilibrium all chemical potentials at the end of the wires are the same and no electric current is driven through the wires. The rates  $\gamma_{wire_j}^{in,out}$  of the generic system are substituted with the rates  $\gamma_{NW_j}^{in,out}$  for the normal wires.

In the case of stationary regime it holds that  $\partial_t P_\uparrow = \partial_t P_\downarrow = \partial_t P_0 = 0$ . This leads to the system of linear equations:

$$0 = (\gamma_{NW_1}^{in} + \gamma_{NW_2}^{in})P_0 - (\gamma_{NW_1}^{out} + \gamma_{NW_2}^{out})P_\uparrow + \gamma_S(P_\downarrow - P_\uparrow) \quad (3.6)$$

$$0 = (\gamma_{NW_1}^{in} + \gamma_{NW_2}^{in})P_0 - (\gamma_{NW_1}^{out} + \gamma_{NW_2}^{out})P_\downarrow + \gamma_S(P_\uparrow - P_\downarrow) \quad (3.7)$$

$$0 = (\gamma_{NW_1}^{out} + \gamma_{NW_2}^{out})P_\uparrow + (\gamma_{NW_1}^{out} + \gamma_{NW_2}^{out})P_\downarrow - (\gamma_{NW_1}^{in} + \gamma_{NW_2}^{in} + \gamma_{NW_1}^{in} + \gamma_{NW_2}^{in})P_0 \quad (3.8)$$

To find the magnetization of the quantum dot, we have to solve eq.(3.6), eq.(3.7) and eq.(3.8) and express  $P_\sigma$  and  $P_0$  in terms of the rates. The solutions can be calculated through standard approach of linear algebra, which yields:

$$P_\uparrow = P_\downarrow = \frac{\gamma_{NW_1}^{in} + \gamma_{NW_2}^{in}}{2(\gamma_{NW_1}^{in} + \gamma_{NW_2}^{in}) + \gamma_{NW_1}^{out} + \gamma_{NW_2}^{out}} \quad (3.9)$$

$$P_0 = \frac{\gamma_{NW_1}^{out} + \gamma_{NW_2}^{out}}{2(\gamma_{NW_1}^{in} + \gamma_{NW_2}^{in}) + \gamma_{NW_1}^{out} + \gamma_{NW_2}^{out}} \quad (3.10)$$



### 3 Main Part

See details in Appendix. The probability for electrons to be in the quantum dot with spin- $\uparrow$  is the same as the probability for electrons with spin- $\downarrow$ . In this case, the spin-flipping rate is completely canceled out of the solutions.

For a system with equal tunneling rates  $\gamma_{NW}^{in,out}$ , it follows that  $P_{\uparrow} = P_{\downarrow} = P_0 \rightarrow \frac{1}{3}$ . For a different system in the limit of high in-tunneling and low out-tunneling rates  $P_{\uparrow} = P_{\downarrow} \rightarrow \frac{1}{2}$  and  $P_0 \rightarrow 0$ . In the limit of high out-tunneling and low in-tunneling rates,  $P_{\uparrow} = P_{\downarrow} \rightarrow 0$  and  $P_0 \rightarrow 1$ , Fig.3.2.

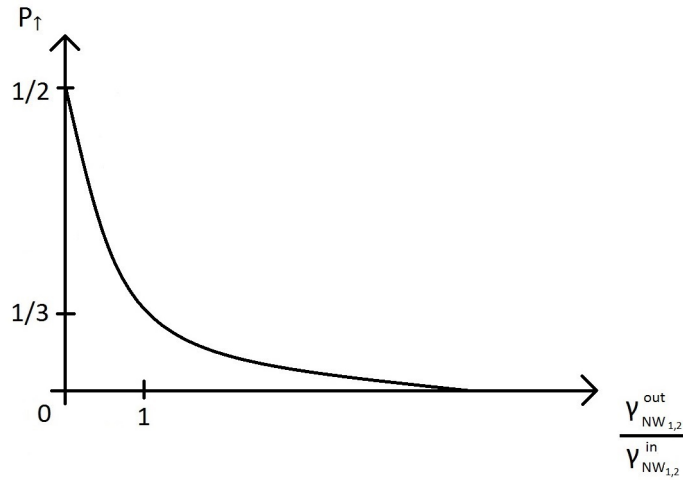


**Figure 3.2:** Probability  $P_{\uparrow}$  depending on the in- and out-tunneling rates either of the normal wire 1 or 2.

### Helical wire-normal wire setup (HW-NW)

In this section, I will consider a helical wire connected to a normal wire via a QD, see Fig.3.3.

The rates  $\gamma_{NW}^{in,out}$  for the normal wire are substituted for the rates  $\gamma_{wire_1}^{in,out}$  of the generic system. Rates for the helical wire  $\gamma_{HW}^{in,out}$  are introduced and substituted for the rates  $\gamma_{wire_2}^{in,out}$  of the generic system. As the helical wire consists of one channel transporting the spin- $\uparrow$  and one channel transporting the spin- $\downarrow$  electrons, a factor  $\frac{1}{2}$  needs to be added to every rate of the helical wire in comparison to a normal wire. These substitutions of rates with the generic system yield the following equations:

### 3 Main Part

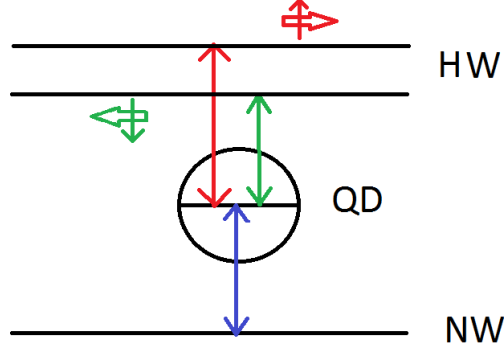


**Figure 3.3:** A scheme of a helical wire (HW) connected to a normal wire (NW) via a QD. The red and green big arrows show the direction in which the electrons can move in the helical wire. The small arrows show the direction of the spin of the electrons in this channel. The long arrows connecting the wires and the QD symbolize the possible tunneling possibilities.

$$\partial_t P_\uparrow = (\gamma_{NW}^{in} + \frac{1}{2}\gamma_{HW}^{in})P_0 - (\gamma_{NW}^{out} + \frac{1}{2}\gamma_{HW}^{out})P_\uparrow + \gamma_S(P_\downarrow - P_\uparrow) \quad (3.11)$$

$$\partial_t P_\downarrow = (\gamma_{NW}^{in} + \frac{1}{2}\gamma_{HW}^{in})P_0 - (\gamma_{NW}^{out} + \frac{1}{2}\gamma_{HW}^{out})P_\downarrow + \gamma_S(P_\uparrow - P_\downarrow) \quad (3.12)$$

$$\begin{aligned} \partial_t P_0 = & (\gamma_{NW}^{out} + \frac{1}{2}\gamma_{HW}^{out})P_\uparrow + (\gamma_{NW}^{out} + \frac{1}{2}\gamma_{HW}^{out})P_\downarrow \\ & - (\gamma_{NW}^{in} + \frac{1}{2}\gamma_{HW}^{in} + \gamma_{NW}^{in} + \frac{1}{2}\gamma_{HW}^{in})P_0 \end{aligned} \quad (3.13)$$

To calculate  $P_\uparrow$ ,  $P_\downarrow$  and  $P_0$  in the stationary regime of the system  $\partial_t P_\uparrow$ ,  $\partial_t P_\downarrow$  and  $\partial_t P_0$  are set to 0. Thus, the following linear system of equations is solved to obtain  $P_\uparrow$ ,  $P_\downarrow$  and  $P_0$  as functions of the rates:

$$0 = (\gamma_{NW}^{in} + \frac{1}{2}\gamma_{HW}^{in})P_0 - (\gamma_{NW}^{out} + \frac{1}{2}\gamma_{HW}^{out})P_\uparrow + \gamma_S(P_\downarrow - P_\uparrow) \quad (3.14)$$

$$0 = (\gamma_{NW}^{in} + \frac{1}{2}\gamma_{HW}^{in})P_0 - (\gamma_{NW}^{out} + \frac{1}{2}\gamma_{HW}^{out})P_\downarrow + \gamma_S(P_\uparrow - P_\downarrow) \quad (3.15)$$

$$0 = (\gamma_{NW}^{out} + \frac{1}{2}\gamma_{HW}^{out})P_\uparrow + (\gamma_{NW}^{out} + \frac{1}{2}\gamma_{HW}^{out})P_\downarrow - (\gamma_{NW}^{in} + \frac{1}{2}\gamma_{HW}^{in} + \gamma_{NW}^{in} + \frac{1}{2}\gamma_{HW}^{in})P_0 \quad (3.16)$$

The solutions obtained through linear algebra are:

### 3 Main Part

$$P_{\uparrow} = P_{\downarrow} = \frac{\gamma_{NW}^{in} + \frac{1}{2}\gamma_{HW}^{in}}{2(\gamma_{NW}^{in} + \frac{1}{2}\gamma_{HW}^{in}) + \gamma_{NW}^{out} + \frac{1}{2}\gamma_{HW}^{out}} \quad (3.17)$$

$$P_0 = \frac{\gamma_{NW}^{out} + \frac{1}{2}\gamma_{HW}^{out}}{2(\gamma_{NW}^{in} + \frac{1}{2}\gamma_{HW}^{in}) + \gamma_{NW}^{out} + \frac{1}{2}\gamma_{HW}^{out}} \quad (3.18)$$

If all rates of the normal and helical wire have the same value,  $P_{\uparrow} = P_{\downarrow} = P_0 \rightarrow \frac{1}{3}$ . In the limit of high in- and low out-tunneling rates,  $P_{\uparrow} = P_{\downarrow} \rightarrow \frac{1}{2}$  and  $P_0 \rightarrow 0$ . In the limit of high out- and low in-tunneling rates it follows that  $P_{\uparrow} = P_{\downarrow} \rightarrow 0$  and  $P_0 \rightarrow 1$ . Hence, there is no difference from previous results.

### Helical wire- helical wire setup (HW-HW)

A model of the last setup is shown in Fig.3.4: two HW are connected via a QD.

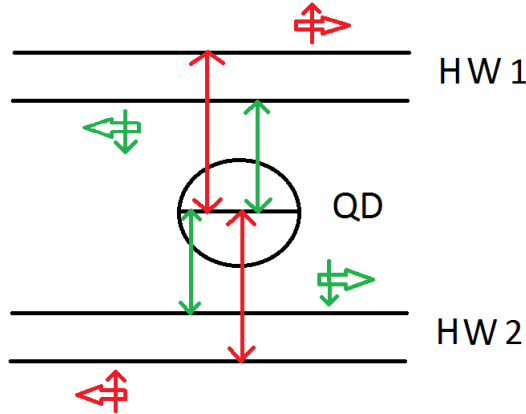


**Figure 3.4:** A scheme of two HW connected via a QD. The red and green big arrows indicate the direction in which the electrons can move in the wires, while the small arrows crossing the wires show the direction of the spin of the electrons in each wire. The long red and green arrows coming and going from each wire to the QD symbolize the possible tunneling processes which can take place.

The rates for the helical wire in the last helical-normal setup are used here for the two wires. As in the first setup, they are labeled to indicate from which wire they are. Substituting them into the rate equations of the generic setup leads to the following equations:

### 3 Main Part

$$\partial_t P_\uparrow = \frac{1}{2}(\gamma_{HW2}^{in} + \gamma_{HW1}^{in})P_0 - \frac{1}{2}(\gamma_{HW2}^{out} + \gamma_{HW1}^{out})P_\uparrow + \gamma_S(P_\downarrow - P_\uparrow) \quad (3.19)$$

$$\partial_t P_\downarrow = \frac{1}{2}(\gamma_{HW1}^{in} + \gamma_{HW2}^{in})P_0 - \frac{1}{2}(\gamma_{HW1}^{out} + \gamma_{HW2}^{out})P_\downarrow + \gamma_S(P_\uparrow - P_\downarrow) \quad (3.20)$$

$$\begin{aligned} \partial_t P_0 &= \frac{1}{2}(\gamma_{HW2}^{out} + \gamma_{HW1}^{out})P_\uparrow + \frac{1}{2}(\gamma_{HW1}^{out} + \gamma_{HW2}^{out})P_\downarrow \\ &\quad - \frac{1}{2}(\gamma_{HW2}^{in} + \gamma_{HW1}^{in} + \gamma_{HW1}^{in} + \gamma_{HW2}^{in})P_0 \end{aligned} \quad (3.21)$$

Note that the structure of the equations is nearly the same as in the NW-NW setup, the factor  $\frac{1}{2}$  is the only difference. The linear system is in the stationary regime,  $\partial_t P_\uparrow = \partial_t P_\downarrow = \partial_t P_0 = 0$ , Eq.(3.19), Eq.(3.20) and Eq.(3.21) result in:

$$0 = \frac{1}{2}(\gamma_{HW2}^{in} + \gamma_{HW1}^{in})P_0 - \frac{1}{2}(\gamma_{HW2}^{out} + \gamma_{HW1}^{out})P_\uparrow + \gamma_S(P_\downarrow - P_\uparrow) \quad (3.22)$$

$$0 = \frac{1}{2}(\gamma_{HW1}^{in} + \gamma_{HW2}^{in})P_0 - \frac{1}{2}(\gamma_{HW1}^{out} + \gamma_{HW2}^{out})P_\downarrow + \gamma_S(P_\uparrow - P_\downarrow) \quad (3.23)$$

$$0 = \frac{1}{2}(\gamma_{HW2}^{out} + \gamma_{HW1}^{out})P_\uparrow + \frac{1}{2}(\gamma_{HW1}^{out} + \gamma_{HW2}^{out})P_\downarrow \quad (3.24)$$

$$-\frac{1}{2}(\gamma_{HW2}^{in} + \gamma_{HW1}^{in} + \gamma_{HW1}^{in} + \gamma_{HW2}^{in})P_0 \quad (3.25)$$

Solving this system with linear algebra leads to the solutions:

$$P_\uparrow = P_\downarrow = \frac{\gamma_{HW1}^{in} + \gamma_{HW2}^{in}}{2(\gamma_{HW1}^{in} + \gamma_{HW2}^{in}) + \gamma_{HW1}^{out} + \gamma_{HW2}^{out}} \quad (3.26)$$

$$P_0 = \frac{\gamma_{HW1}^{out} + \gamma_{HW2}^{out}}{2(\gamma_{HW1}^{in} + \gamma_{HW2}^{in}) + \gamma_{HW1}^{out} + \gamma_{HW2}^{out}} \quad (3.27)$$

These formulas look exactly as in the case of the two normal wires coupled via a QD. As in the NW-NW setup, for equal values of the tunneling rates the probabilities for electrons in the quantum dot are  $P_\uparrow = P_\downarrow = P_0 = \frac{1}{3}$ . In the different limits of in- and out- tunneling rates, the same results are obtained as in the case of the NW-NW setup. Thus, we see no difference between helical- and normal-helical configurations in equilibrium.

Calculating the probabilities for electrons with a different spin to be in the QD shows no magnetization in equilibrium regardless of the wire helicity.

### 3.3 Solution of rate equations for different setups out of equilibrium

#### Biasing the normal wires

Biasing the normal wires through different chemical potentials at their end would introduce an electric current flowing through the wire. This modification changes the different rates for electrons tunneling from the wires to the QD or from the QD to the wires as less channels contribute to the system, Fig.3.5. Thus, the rates become smaller. But this does not change the equivalence  $P_{\uparrow} = P_{\downarrow}$  as seen in the previous part.

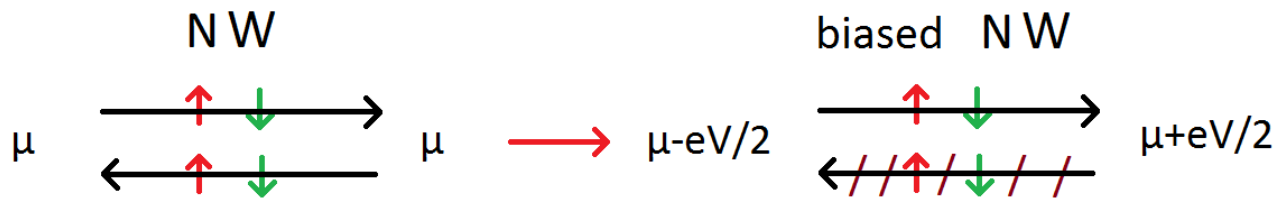


**Figure 3.5:** The varied chemical potentials introduce an electric current, which effectively disables the left-moving channel. Thus, the biased NW has less channels contributing to the system compared with an unbiased NW.

#### Biasing the helical wires

Different chemical potentials  $\mu$  at the ends of the helical wires lead although to a electric current flowing through the wire. This current drives through one of the two channels either the right moving or the left moving, depending on the applied chemical potentials. The other channel is effectively disabled. Due to the helicity of the wire, the motion direction of the electrons is coupled to their spin and if one channel is disabled no electrons with the spin of this channel are involved in the tunneling, Fig.3.6.

Thus, there is not only a charge but also a spin current. The rate equations for a setup with this kind of biased helical wire miss both, the in- and the out-tunneling rates, as they drop out of the equations due to the disabled channel.

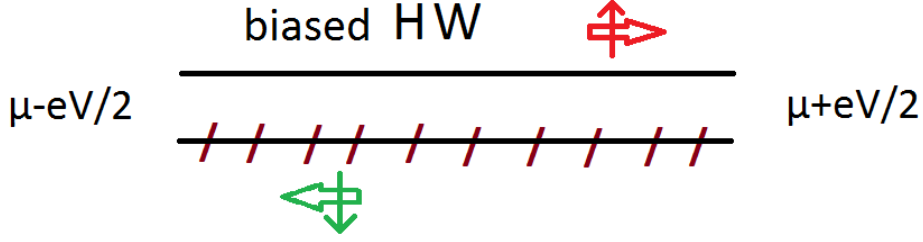


**Figure 3.6:** The chemical potential at the end of the helical wire is varied to  $\mu - eV/2$  at the left and  $\mu + eV/2$  at the right, introducing an electric current through the right moving channel. The left moving channel is effectively disabled due to this.

### Biased HW-NW setup

The chemical potential disables the left moving channel with the spin- $\downarrow$  electrons in the HW-NW setup. The rate equations, Eqs.(3.11), (3.12) and (3.13), differ from the unbiased setup, as the rates  $\frac{1}{2}\gamma_{HEW}^{in,out}$  are zero for spin- $\downarrow$  channel. Substituting 0 for them and calculating the linear system of equations for  $\partial_t P_\uparrow = \partial_t P_\downarrow = \partial_t P_0 = 0$  leads to the solutions:

$$P_\uparrow = \frac{\gamma_{NW}^{in} + \frac{1}{2}\gamma_{HW}^{in}}{2(\gamma_{NW}^{in} + \frac{1}{4}\gamma_{HW}^{in}) + \gamma_{NW}^{out} + \frac{1}{4}\gamma_{HW}^{out}} \quad (3.28)$$

$$P_\downarrow = \frac{\gamma_{NW}^{in}}{2(\gamma_{NW}^{in} + \frac{1}{4}\gamma_{HW}^{in}) + \gamma_{NW}^{out} + \frac{1}{4}\gamma_{HW}^{out}} \quad (3.29)$$

$$P_0 = \frac{\gamma_{NW}^{out} + \frac{1}{4}\gamma_{HW}^{out}}{2(\gamma_{NW}^{in} + \frac{1}{4}\gamma_{HW}^{in}) + \gamma_{NW}^{out} + \frac{1}{4}\gamma_{HW}^{out}} \quad (3.30)$$

Setting all rates to an equal value results in  $P_\uparrow \rightarrow \frac{3}{5}$ ,  $P_\downarrow \rightarrow \frac{4}{15}$  and  $P_0 \rightarrow \frac{1}{3}$ , clearly identifying an accumulation of spins with a spin- $\uparrow$  in the quantum dot, Fig.3.7. Thus, we have shown that the QD obtains a finite magnetization in the case of a biased HW connected to a NW via a QD, which is the manifestation of the helicity.

### 3 Main Part

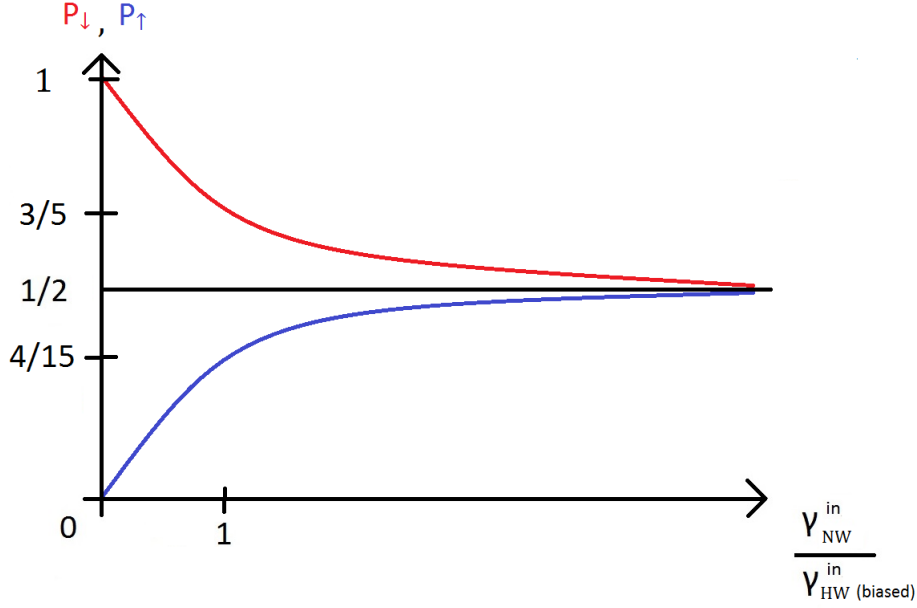


**Figure 3.7:** Probabilities  $P_\sigma$  depending on the in-tunneling rates of the NW and the biased HW.

The analysis and results are the same when the right moving channel with the spin- $\uparrow$  electrons is disabled. The probability  $P_\downarrow$  increases as the rates for spin- $\uparrow$  electrons,  $\frac{1}{2}\gamma_{HW}^{in,out}$ , drop out of the equations.

### Biased HW-HW setup

Similar to the previous section different chemical potentials are used to induce an electric current through a helical wire by effectively disabling one channel. In the first case, the right moving channel of the HW1, Fig.3.4, is disabled and the rates  $\frac{1}{2}\gamma_{HW1}^{in,out}$  for spin- $\uparrow$  electrons are zero. Calculating  $P_\uparrow$ ,  $P_\downarrow$  and  $P_0$  for  $\partial_t P_\uparrow = \partial_t P_\downarrow = \partial_t P_0 = 0$ , leads to:

$$P_\uparrow = \frac{\gamma_{HW2}^{in}}{2(\frac{1}{2}\gamma_{HW1}^{in} + \gamma_{HW2}^{in}) + \frac{1}{2}\gamma_{HW1}^{out} + \gamma_{HW2}^{out}} \quad (3.31)$$

$$P_\downarrow = \frac{\gamma_{HW1}^{in} + \gamma_{HW2}^{in}}{2(\frac{1}{2}\gamma_{HW1}^{in} + \gamma_{HW2}^{in}) + \frac{1}{2}\gamma_{HW1}^{out} + \gamma_{HW2}^{out}} \quad (3.32)$$

### 3 Main Part

$$P_0 = \frac{\frac{1}{2}\gamma_{HW1}^{out} + \gamma_{HW2}^{out}}{2(\frac{1}{2}\gamma_{HW1}^{in} + \gamma_{HW2}^{in}) + \frac{1}{2}\gamma_{HW1}^{out} + \gamma_{HW2}^{out}} \quad (3.33)$$

If all rates are set at an equal value,  $P_0 \rightarrow \frac{1}{3}$  and  $P_\uparrow \rightarrow \frac{2}{9}$  as  $P_\downarrow \rightarrow \frac{4}{9}$ . Clearly identifying a magnetization in the quantum dot, Fig.3.8.

The same results are obtained due to the symmetry of the system, when the  $\uparrow$ -channel of the second helical wire is disabled and the  $\uparrow$ -channel for the first wire is unbiased. Disabling one  $\downarrow$ -channel in either the upper or the lower wire leads to the same results, Fig.3.8.

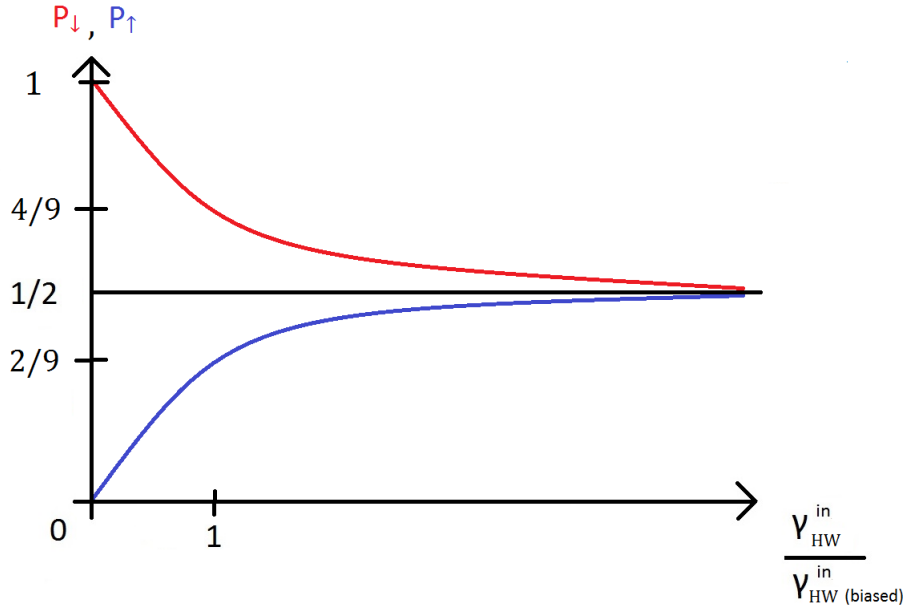


**Figure 3.8:** Probabilities  $P_\sigma$  depending on the in-tunneling rates of the HW and the biased HW.



## 4 Conclusion

In this thesis, I examined the tunneling of electrons between normal- and helical-wires connected via a quantum dot. Rate equations were derived to describe the probabilities of electrons with a given spin to be in the QD. The goal was to investigate the magnetization of the QD. Rate equations were constructed in the setups of two normal wires, a helical and a normal wire and two helical wires connected via a QD. I have considered equilibrium and non-equilibrium cases. In the latter regime, the helical wire is biased which effectively disables one of their channels. This produces to a chiral wire, where conduction electrons have only one given spin state.

For all three setups no magnetization was found in the case of equilibrium, regardless of particular values of rates.

Out of equilibrium, an electric current is driven through the biased helical wire. The current is provided by the electrons with a given helicity; the second helical channel is suppressed if the bias is strong enough. A finite magnetization of the QD was found in the cases of biased helical wires connected with a normal wire or another helical wire via a QD.

This magnetization is a direct manifestation of the helicity of the biased wire and can be used in real experiments to detect the helical wires. The calculation of the magnetization is a first step and further investigation should be done calculating the current, induced in the unbiased wire via tunneling.

## 5 Appendix: Calculation of $P_{\uparrow}, P_{\downarrow}$ and $P_0$

In this section I show how the probabilities  $P_{\uparrow}, P_{\downarrow}$  and  $P_0$  are calculated for the different setups. Of course more than one way leads to the solutions.

I start with the NW-NW setup and its system of linear equations:

$$0 = (\gamma_{NW_1}^{in} + \gamma_{NW_2}^{in})P_0 - (\gamma_{NW_1}^{out} + \gamma_{NW_2}^{out})P_{\uparrow} + \gamma_S(P_{\downarrow} - P_{\uparrow}) \quad (5.1)$$

$$0 = (\gamma_{NW_1}^{in} + \gamma_{NW_2}^{in})P_0 - (\gamma_{NW_1}^{out} + \gamma_{NW_2}^{out})P_{\downarrow} + \gamma_S(P_{\uparrow} - P_{\downarrow}) \quad (5.2)$$

$$0 = (\gamma_{NW_1}^{out} + \gamma_{NW_2}^{out})P_{\uparrow} + (\gamma_{NW_1}^{out} + \gamma_{NW_2}^{out})P_{\downarrow} - (\gamma_{NW_1}^{in} + \gamma_{NW_2}^{in} + \gamma_{NW_1}^{in} + \gamma_{NW_2}^{in})P_0 \quad (5.3)$$

I take Eq.(5.1) and subtract Eq.(5.2), leading to

$$0 = (\gamma_{NW_1}^{out} + \gamma_{NW_2}^{out})P_{\downarrow} - (\gamma_{NW_1}^{out} + \gamma_{NW_2}^{out})P_{\uparrow} + 2\gamma_S(P_{\downarrow} - P_{\uparrow}). \quad (5.4)$$

After repositioning after  $\frac{P_{\uparrow}}{P_{\downarrow}}$  and cancelling the equal terms it states:

$$\frac{P_{\uparrow}}{P_{\downarrow}} = 1 \quad (5.5)$$

Now Eq.(5.3) is repositioned after  $P_0$  and the result  $P_{\uparrow} = P_{\downarrow} \equiv P_{\uparrow,\downarrow}$  is plugged into the second equivalence sign, leading to:

$$P_0 = \frac{\gamma_{NW_1}^{out} + \gamma_{NW_2}^{out}}{2(\gamma_{NW_1}^{in} + \gamma_{NW_2}^{in})} (P_{\uparrow} + P_{\downarrow}) = \frac{\gamma_{NW_1}^{out} + \gamma_{NW_2}^{out}}{\gamma_{NW_1}^{in} + \gamma_{NW_2}^{in}} P_{\uparrow,\downarrow} \quad (5.6)$$

With the result of Eq.(5.5) plugged into Eq.(3.1) it follows that

## 5 Appendix: Calculation of $P_{\uparrow}, P_{\downarrow}$ and $P_0$

$$P_0 = 1 - (P_{\uparrow} + P_{\downarrow}) = 1 - 2P_{\uparrow, \downarrow} \quad (5.7)$$

Now Eq.(5.6) and Eq.(5.7) are equivalent leading to

$$1 - 2P_{\uparrow, \downarrow} = \frac{\gamma_{NW_1}^{out} + \gamma_{NW_2}^{out}}{\gamma_{NW_1}^{in} + \gamma_{NW_2}^{in}} P_{\uparrow, \downarrow} \quad (5.8)$$

Repositioning after  $P_{\uparrow, \downarrow}$  leads to the result Eq.(3.9) and to Eq.(3.10) if plugged into Eq.(5.6). This is one way how the NW-NW solutions are obtained.

The results for the other setups HW-NW and HW-HW in the equilibrium can be calculated the same way just with different rates in the equations. Or through remaining the rates in the solutions in the NW-NW case.

The solutions for the biased systems can be obtained through calculating the linear systems of equations in which the rates for the disabled channels are set to 0 or by setting the same rates in the equations for the solutions in the equilibrium to 0.

## 6 Acknowledgements

I would like to thank the LS von Delft for the extraordinary working conditions and for the good working atmosphere. This thesis was written by myself but would have never been possible without the help of Dr.Oleg Yevtushenko who offered this thesis and always helped with great afford in every possible way. It was a pleasure and grand opportunity to learn from his experience and his skills.

# Bibliography

- [1] C. Kane and C. K. Hasan, "Colloquium: Topological insulators," *Rev. Mod. Phys.*, **82**, 3045, (2010).
- [2] B. Rizzo, A. Camjayi, and L. Arrachea, "Transport in quantum spin Hall edges in contact to a quantum dot," *Phys. Rev. B*, **94**, 125425, (2016).
- [3] C. Kane and E. J. Mele, " $Z_2$  Topological Order and the Quantum Spin Hall Effect," *Phys. Rev. Lett.*, **95**, 146802, (2005).
- [4] M. Autore, *Terahertz and Infrared study of topological insulators*. PhD thesis, Sapienza - Universita di Roma, (2015).
- [5] M. König *et al.*, "Quantum Spin Hall Insulator in HgTe Quantum Wells," *Science*, **318**, 766-770 (2007).
- [6] A. M. Tselik and O. M. Yevtushenko, "Quantum Phase Transition and Protected Ideal Transport in a Kondo Chain," *Phys. Rev. Lett.*, **115**, 216402, (2015).
- [7] D. H. Schimmel, A. M. Tselik, and O. M. Yevtushenko, "Low energy properties of the Kondo chain in the RKKY regime," *New J. of Phys.*, **18**, 053004, (2016).
- [8] N. Andrei, K. Furuya, and J. H. Lowenstein, "Solution of the Kondo problem," *Rev. Mod. Phys.*, **55**, 331, (1983).
- [9] G. Grüner, "The dynamics of charge-density waves," *Rev. Mod. Phys.*, **60**, 1129 (1988).
- [10] C. H. L. Quay *et al.*, "Observation of a one-dimensional spin-orbit gap in a quantum wire," *Nature Physics*, **6**, 336-339, (2010).
- [11] C. P. Scheller *et al.*, "Evidence for Helical Nuclear Spin Order in GaAs Quantum Wires," *Phys. Rev. Lett.*, **112**, 066801, (2014).

## Bibliography

- [12] D. Loss, "Nuclear magnetism and electron order in interacting one-dimensional conductors," *Phys. Rev. B*, **80**, 165119, (2009).
- [13] T. Ando, A. B. Fowler, and F. Stern, "Electronic properties of two-dimensional systems," *Rev. Mod. Phys.*, **54**, 437, (1982).
- [14] Y. V. Nazarov and Y. M. Blanter, *Quantum Transport*. Cambridge University Press, (2009).
- [15] I.L.Aleiner, P. Brouwer, and L. Glazman, "Quantum effects in Coulomb blockade," *Phys. Reports*, **358**, 309-440, (2002).
- [16] X.-L. Qi, "Topological insulators and superconductors," *Rev. Mod. Phys. B*, **83**, 1057, (2011).
- [17] Y. Tanaka, A. Furusaki, and K. Matveev, "Conductance of a helical edge liquid coupled to a magnetic impurity," *Phys. Rev. Lett.*, **106**, 236402, (2011).

# Eidesstattliche Erklärung

Hiermit versichere ich, dass ich die vorliegende Arbeit selbstständig verfasst und keine anderen als die angegebenen Quellen und Hilfsmittel benutzt habe, dass alle Stellen der Arbeit, die wörtlich oder sinngemäß aus anderen Quellen übernommen wurden, als solche kenntlich gemacht und dass die Arbeit in gleicher oder ähnlicher Form noch keiner Prüfungsbehörde vorgelegt wurde.

Ort, Datum

Unterschrift